



A Journal of the Gesellschaft Deutscher Chemiker

Angewandte Chemie

GDCh

International Edition

www.angewandte.org

Accepted Article

Title: Solar-Powered Organic Semiconductor-Bacteria Biohybrids for CO₂ Reduction into Acetic Acid

Authors: Shu Wang

This manuscript has been accepted after peer review and appears as an Accepted Article online prior to editing, proofing, and formal publication of the final Version of Record (VoR). This work is currently citable by using the Digital Object Identifier (DOI) given below. The VoR will be published online in Early View as soon as possible and may be different to this Accepted Article as a result of editing. Readers should obtain the VoR from the journal website shown below when it is published to ensure accuracy of information. The authors are responsible for the content of this Accepted Article.

To be cited as: *Angew. Chem. Int. Ed.* 10.1002/anie.202001047
Angew. Chem. 10.1002/ange.202001047

Link to VoR: <http://dx.doi.org/10.1002/anie.202001047>
<http://dx.doi.org/10.1002/ange.202001047>

Solar-Powered Organic Semiconductor-Bacteria Biohybrids for CO₂ Reduction into Acetic Acid

Panpan Gai^{a,b}, Wen Yu^{a,b}, Hao Zhao^{a,c}, Ruilian Qi^a, Feng Li^{*b}, Libing Liu^a, Fengting Lv^a, Shu Wang^{*a, c}

Abstract: Photosynthetic biohybrid systems have emerged as a promising platform for solar-to-chemical conversion by integrating excellent light-harvesting ability of semiconductors with the synthetic capability of biological cells. How to enhance the utilization of solar energy, hole/electron separation efficiency and the electron transfer between the semiconductor and biological cells is crucial to develop high-performance photosynthesis platforms. In this work, we developed an organic semiconductor-bacteria biohybrid photosynthetic system, which could efficiently realize CO₂ reduction to produce acetic acid through non-photosynthetic bacteria *Moorella thermoacetica*. As the photosensitizers, both cationic electron-transporting (*n*-type) perylene diimide derivative (PDI) and hole-transporting (*p*-type) poly(fluorene-co-phenylene) (PFP) were coated on the bacteria surface to form *p-n* heterojunction (PFP/PDI) layer, affording higher hole/electron separation efficiency. The π -conjugated semiconductors possess excellent light-harvesting ability and biocompatibility, and more importantly, the cationic side chains of organic semiconductors could intercalate into cell membrane, ensuring the efficient electron transfer to bacteria. As a result, *Moorella thermoacetica* can harvest photoexcited electrons from the PFP/PDI heterojunction, which can drive the Wood-Ljungdahl pathway to synthesize acetic acid from CO₂ under illumination. The efficiency of this organic biohybrid is ~ 1.6 %, which is comparable to those of reported inorganic biohybrid systems. This work opens a new avenue to explore bioenergy application of organic semiconductors, and also provides a convenient biomanufacturing approach to design organic semiconductor-bacteria biohybrids for efficient solar-to-chemical conversion.

As one emerging technology, photosynthetic biohybrid systems are considered as the promising chemical synthesis platform by taking advantage of excellent light-harvesting ability of semiconductors and the synthetic ability of biological cells or bioenzyme.^[1,2] Versatile solar-to-chemical production have been investigated, including cofactor regeneration,^[3-5] CO₂

reduction,^[6-9] hydrogen production,^[10,11] and dinitrogen fixation,^[12] etc. Among them, compared with that of the bioenzyme, the whole-cell strategy has the advantages of self-replicate and self-repair, as well as the involvement of the complete biological process.^[8,9] In the biological cell-based photosynthetic biohybrid systems, the main light-harvesting materials are generally the inorganic semiconductors, such as cobalt phosphate (CoP),^[3] indium phosphide (InP),^[6] cadmium sulfide (CdS),^[7,12] and gold nanoclusters (AuNCs).^[8] However, in terms of the inorganic semiconductors, the toxicity of heavy metals and phototoxicity to organisms are unfavorable for photosynthetic biohybrid systems. In addition, the optical property of inorganic semiconductors was also difficult to regulate. Thus, how to enhance the solar energy capture ability, hole/electron separation efficiency and the electron transfer from the semiconductor to microorganisms is crucial to develop high-performance photosynthesis platforms.^[1]

Organic semiconductors, especially π -conjugated molecules, aroused our interest because of their good biocompatibility to organisms in versatile biological system,^[13-15] desirable photoelectronic conversion capacity in electrochemical devices,^[16,17] as well as the fine-tuned frontier molecular orbital energy levels and optical band gap.^[18,19] Very recently, the conjugated polymers have been found to exhibit the ability to accelerate electron transfer to thylakoid, leading to the enhancement of the photosynthesis of chloroplasts.^[20,21] More importantly, cationic conjugated polymers can greatly enhance extracellular electron transport exoelectrogen to the electrode by intercalating into the membrane of bacteria through electrostatic interactions and hydrophobic interactions.^[22] Thus, it can be seen that organic conjugated semiconductors could provide an excellent opportunity to develop efficient solar-to-chemical conversion biohybrid systems. To the best of our knowledge, organic semiconductor-bacteria biohybrid photosynthetic system has not been explored up to date. In this work, we developed an organic semiconductor-bacteria biohybrid photosynthetic system, which could efficiently realize CO₂ reduction to produce acetic acid through non-photosynthetic bacteria *Moorella thermoacetica* (*M. thermoacetica*, ATCC 39073). Taking advantage of good solar energy capture ability of π -conjugated molecules, excellent biocompatibility, good hole/electron separation efficiency of *p-n* heterojunction of PFP/PDI pair and the enhanced electron transfer from PFP/PDI to *M. thermoacetica*, this biohybrid system could efficiently realize CO₂ reduction to produce acetic acid under light illumination with an efficiency of 1.6 %.

Scheme 1a shows the diagram of the PDI/PFP/*M. thermoacetica* photosynthesis biohybrid system. To enhance the hole/electron separation efficiency, the *p-n* heterojunction layer composed of cationic PDI and PFP was served as the photosensitizer through simultaneously coating them onto the bacteria surface. Furthermore, it was found that PDI and PFP interacted with *M. thermoacetica* by electrostatic interactions and their cationic side chains could intercalate into cell

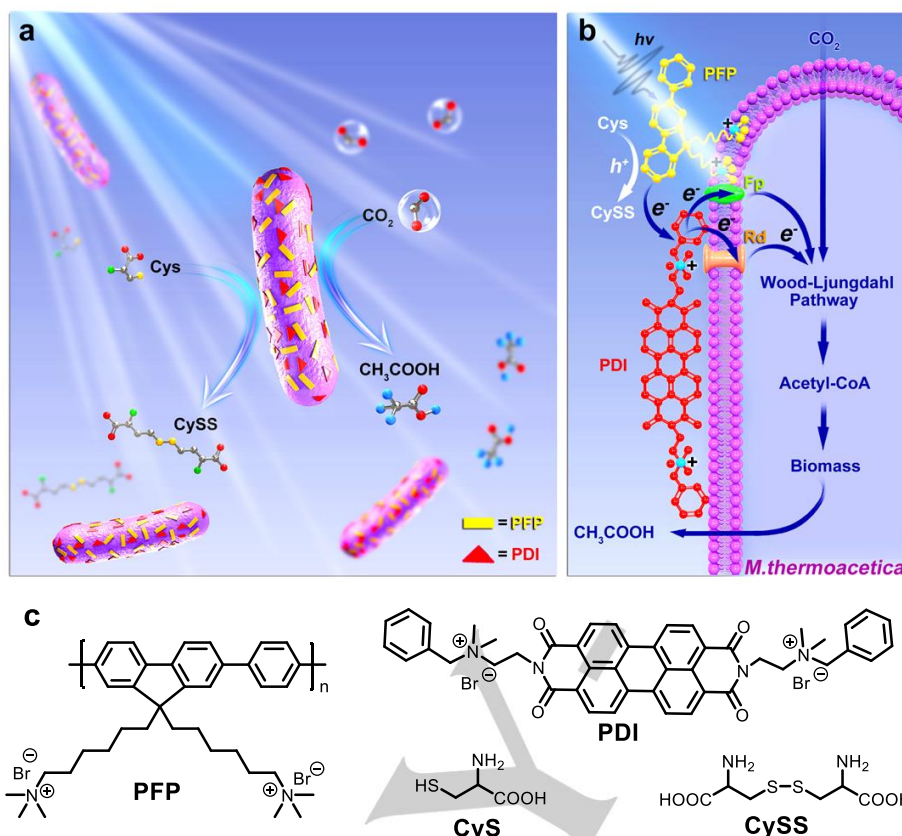
[a] Prof. S. Wang, Dr. L. Liu, Dr. F. Lv, Dr. P. Gai, W. Yu, H. Zhao, R. Qi

Beijing National Laboratory for Molecular Sciences, Key Laboratory of Organic Solids, Institute of Chemistry, Chinese Academy of Sciences, Beijing 100190, P. R. China.
E-mail: wangshu@iccas.ac.cn

[b] Prof. F. Li, Dr. P. Gai, W. Yu
College of Chemistry and Pharmaceutical Sciences, Qingdao Agricultural University, Qingdao 266109, P. R. China.
E-mail: lifeng@qau.edu.cn

[c] Prof. S. Wang, H. Zhao
College of Chemistry, University of Chinese Academy of Sciences, Beijing 100049, P. R. China

Supporting information for this article is given via a link at the end of the document.



Scheme 1. Schematic diagram of the PDI/PFP/*M. thermoacetica* photosynthesis hybrid system (a) and the photoexcited electron generated from PDI/PFP under illumination transferred by the membrane protein and finally passed on to the Wood-Ljungdahl pathway for CO₂ reduction (b). (c) The chemical structures of PFP, PDI, Cys and CySS.

membrane by hydrophobic interactions. This unique feature could ensure the efficient electron transfer to bacteria and circumvent the extra energy consumption when redox shuttles transmembrane transport. As a result, *M. thermoacetica* can harvest photoexcited electrons from the PFP/PDI heterojunction, which drives the Wood-Ljungdahl pathway to synthesize acetic acid from CO₂ under illumination (**Scheme 1b**).

To check the successful construction of the *p-n* heterojunction layer on the surface of *M. thermoacetica*, photocurrent responses of PFP, PDI and PDI/PFP were carried out. Compared to that of PDI with anodic photocurrent (**Figure 1a**) and PFP with cathodic photocurrent (**Figure 1b**), PDI/PFP heterojunction exhibited significantly higher anodic photocurrent (**Figure 1c**), which indicated that *p-n* heterojunction structure was beneficial to hole/electron separation efficiency. This could also be verified from the appropriate cascade energy level of PDI and PFP calculated by electrochemical and spectrographic measurements (**Figure S1** and **Figure 1d**). Both HOMO and LUMO energy level offset between these two molecules exceeded 0.3 eV (1.29 eV for ΔE_{LUMO} and 0.48 eV for ΔE_{HOMO}), which can provide enough driving force for hole/electron dissociation.^[23]

To clarify the interaction between PDI and/or PFP and *M. thermoacetica*, isothermal titration microcalorimetry (ITC) was carried out to examine the thermodynamic changes during the binding process of *M. thermoacetica* with the conjugated molecules.^[24-25] As shown in **Figure 2a**, when PDI or/and PFP was titrated into *M. thermoacetica* solution, the observed enthalpy (ΔH_{obs}) curves exhibited obviously different trend with

the change from negative to zero for PDI/*M. thermoacetica* and from a largely positive value to zero for PFP/*M. thermoacetica*, owing to the different binding modes. In detail, the binding of PDI and *M. thermoacetica* was an exothermic process mainly caused by the electrostatic interactions between the cationic quaternary ammonium groups of PDI and the negative charged surface of *M. thermoacetica*. By contrast, the endothermic binding between PFP and *M. thermoacetica* was mainly attributed to PFP inserting into bacterial membrane through hydrophobic interactions followed by electrostatic adsorption on the bacteria surface. With the addition of PDI/PFP mixture, ΔH_{obs} was still positive but obviously smaller than that of PFP, which suggested the coexistence of the aforementioned interactions. Furthermore, the binding constant K_a of PDI/PFP/*M. thermoacetica* ($8.72 \times 10^5 \text{ M}^{-1}$) calculated by the fitting ITC curve was significantly larger than that of PDI/*M. thermoacetica* ($3.34 \times 10^5 \text{ M}^{-1}$) and PFP/*M. thermoacetica* ($7.73 \times 10^4 \text{ M}^{-1}$), implying the PDI/PFP mixture possessed stronger bioaffinity towards *M. thermoacetica* to form *p-n* heterojunction layer on the bacteria surface.

Apart from the ITC measurement, zeta (ζ) potentials were also measured to confirm the interaction of conjugated molecules and *M. thermoacetica* (**Figure 2b**). Initially, ζ potentials of separated *M. thermoacetica*, PDI, PFP, and PDI/PFP were -38.5 ± 0.7 , 31.3 ± 1.2 , 21.6 ± 1.5 , and 25.2 ± 0.5 mV, respectively. When incubated with PDI, the ζ potential of *M. thermoacetica* presented an obvious positive shift to -32.2 ± 0.2 mV, indicating that PDI bounded to the surface of

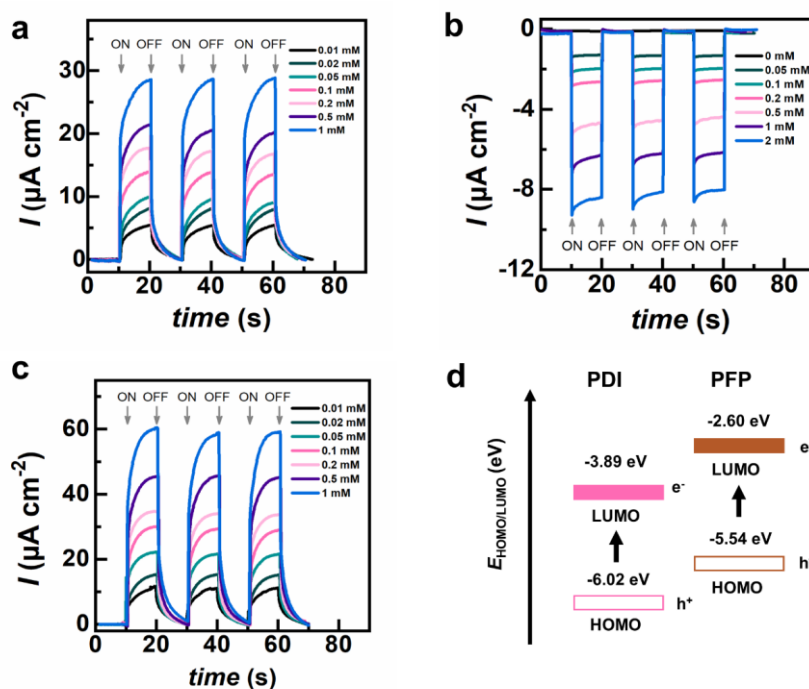


Figure 1. Representative photocurrent responses of PDI (a), PFP (b), PDI/PFP heterojunction (c) on a carbon paper electrode with the interval of 10 s, which were recorded at 0 V bias in phosphate buffer (0.1 M, pH=7.4) containing 0.1 M cysteine as the electron donor. (c) Energy level diagram of PDI and PFP.

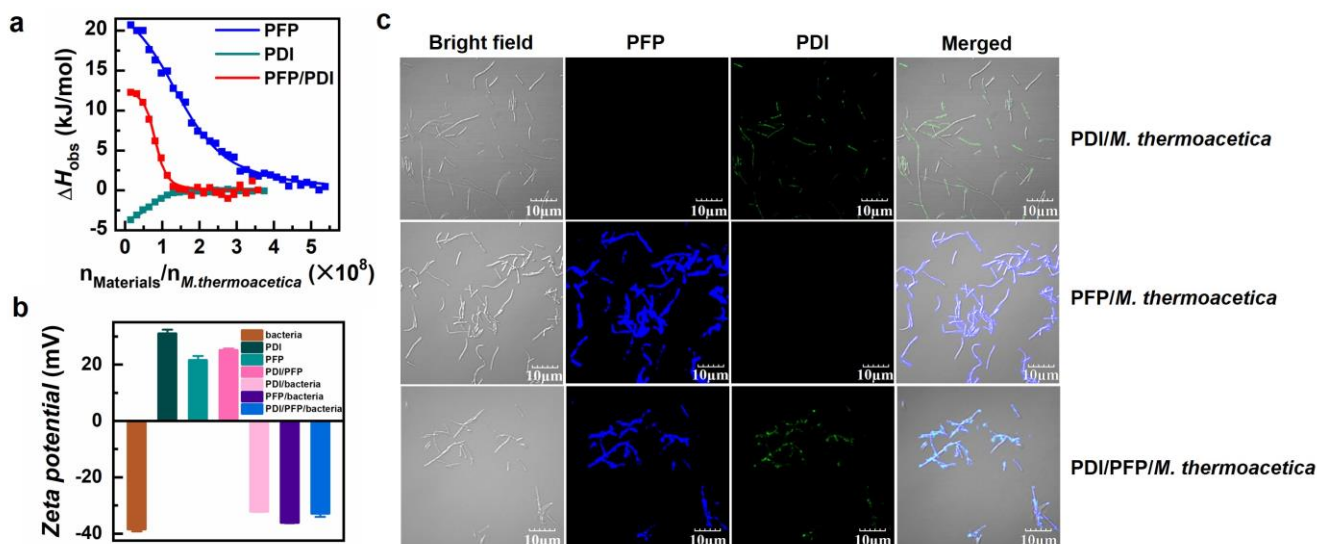


Figure 2. (a) The variation of observed enthalpy changes (ΔH_{obs}) against PDI/*M. thermoacetica*, PFP/*M. thermoacetica*, PDI/PFP/*M. thermoacetica* ratio by titrating PDI, PFP, PDI/PFP, respectively. (b) Zeta potentials of *M. thermoacetica*, PDI, PFP, PDI/PFP, PDI/*M. thermoacetica*, PFP/*M. thermoacetica*, PDI/PFP/*M. thermoacetica*, respectively. (c) CLSM images of *M. thermoacetica* incubated with PDI, PFP and PDI/PFP (10 μM) for 2 h. To avoid the crossover of PDI and PFP, for PDI, the excitation wavelength was 559 nm and the fluorescence images were collected the signals from 580-680 nm. For PFP, the excitation wavelength was 405 nm and the fluorescence images were collected the signals from 425-475 nm.

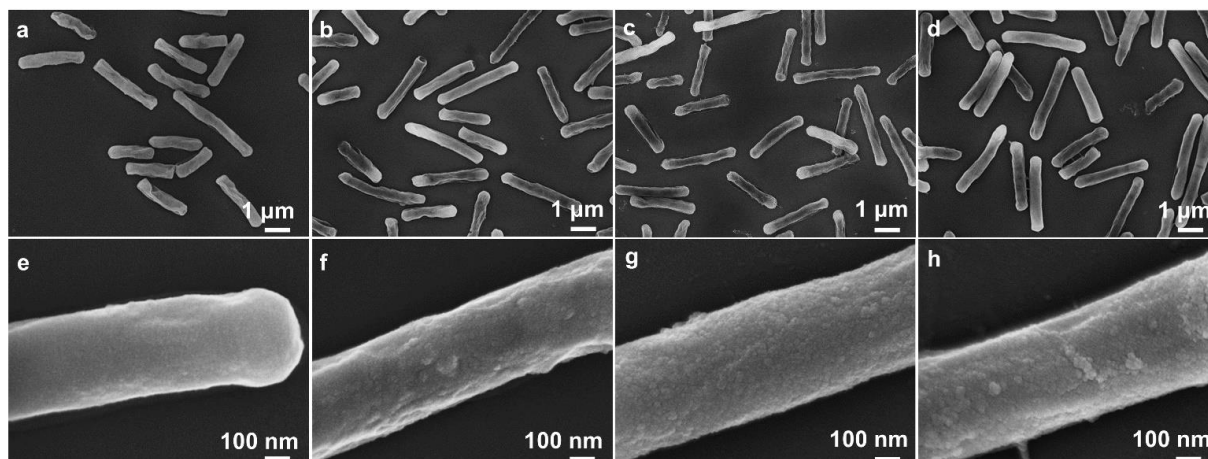


Figure 3. SEM images of *M. thermoacetica* (a,e), PFP/*M. thermoacetica* (b,f), PDI/*M. thermoacetica* (c,g), PDI/PFP/*M. thermoacetica* (d,h). (e), (f), (g) and (h) were the enlarged images of (a), (b), (c) and (d), respectively.

M. thermoacetica through electrostatic interactions. By contrast, PFP/*M. thermoacetica* displayed a slight increase of ζ potentials to -36.2 ± 0.1 mV, suggesting that the positively charged side chain in PFP intercalated into bacterial membrane.^[26, 27] After PDI/PFP mixture interacted with *M. thermoacetica*, the ζ potential was up-shifted to -32.9 ± 1.1 mV, owing to the co-existed electrostatic and hydrophobic interactions. To obtain a more straightforward understanding of the interaction between the conjugated molecules and *M. thermoacetica*, confocal laser scanning microscope (CLSM) imaging and scanning electron microscopy (SEM) were conducted for *M. thermoacetica* incubated with PDI, PFP and PDI/PFP mixture. From CLSM images as shown in **Figure 2c**, it can be observed that PDI and PFP well localized at the surface of bacteria, accompanying with green and blue fluorescence, respectively. As expected, *M. thermoacetica* incubated with PDI/PFP could simultaneously present green and blue fluorescence, indicating their co-binding towards bacteria surface. The same results were also confirmed by SEM images. As shown in **Figure 3**, Compared to that of neat *M. thermoacetica*, the surface of *M. thermoacetica* incubated with PDI, PFP and PDI/PFP mixture turned obviously rough. In other words, the conjugated molecules could be uniformly coated on the bacteria surface. Furthermore, PDI/PFP/*M. thermoacetica* and PDI/*M. thermoacetica* or PFP/*M. thermoacetica* were also in good shape, suggesting that the good biocompatibility between the conjugated molecules and bacteria.

We investigated the photosynthetic ability of the biohybrid system, in which, the product acetic acid was monitored by quantitative proton nuclear magnetic resonance (H-NMR). To study the photosynthetic behavior, the biohybrid system was performed in the illumination of light-dark cycle of 12 hours each to imitate the intermittent nature of the solar source. **Figure 4a-4c** shows that in the two deletional controls, namely *M. thermoacetica* in the light and conjugated molecules/*M. thermoacetica* in the dark, the concentration of the acetic acid was only ~ 0.1 mM, which might be the accumulation under the initial autotrophic acclimation. Under light illumination, conjugated molecules/*M. thermoacetica* could exhibit apparent production of the acetic acid. As expected, the accumulated acetic acid yield of PDI/PFP/*M. thermoacetica* (~ 0.63 mM) was significantly higher than that of PDI/*M. thermoacetica* (~ 0.25

mM) or PFP/*M. thermoacetica* (~ 0.4 mM) under the same conditions (**Figure 4a** and **Figure S2**). The noticeable increase was attributed to the efficient hole/electron separation and good affinity of the PDI/PFP mixture towards bacteria surface. Furthermore, the effect of illumination intensity and conjugated molecule concentration on the efficiency of solar-to-chemical conversion was investigated. The low power density could reduce the photogenerated hole-electron pair while excessive illumination intensity might result in the complete destruction of the cell membrane, thus, the optimal light power density was 5.0 mW/cm². Meanwhile, the PDI/PFP concentration was also critical for the photosynthesis of the biohybrid system. When the concentration of the PDI/PFP was 10 μ M, the maximum amount of the acetic acid produced (**Figure S3**), which could be ascribed to excessive holes formed in the bacterial surface destructing cell membrane. To furthermore study the photosynthetic behavior, the produced acetic acid amount of PDI/PFP/*M. thermoacetica* was monitored in an alternating light-dark cycle of 12 hours each. Because of the accumulation of metabolic intermediates, acetic acid was continuously produced during the day-night cycles, which was also confirmed by previous studies.^[7,8] At the third day, the accumulation amount of the acetic acid was 0.63 mM. Eventually, the quantum yield of 1.6% was calculated based on the initial Cys concentration (the details in supporting information), which was comparable to the year-long averages determined for plants and algae as well as the inorganic biohybrid system ranging from ~ 0.2 to 2.8% .^[3,6-8,28] Noticeably, during the photosynthesis, the cell number of *M. thermoacetica* in the presence of PDI/PFP increased to $\sim 300\%$ after 3 days while that of *M. thermoacetica* in the control group did not (**Figure S4**). This result suggested that PDI/PFP could promote the growth of bacteria and exhibit good biocompatibility.

To clarify the mechanism of photoexcited electron transfer, cyclic voltammetry (CV) was performed for *M. thermoacetica* incubated with PDI/PFP (**Figure 4d**). The separated *M. thermoacetica* has a couple of redox peaks at -0.2 V and a reduction peak at -0.5 V, which might be attributed to the redox mediators rubredoxins (Rd) and flavoproteins (Fp) distributed on the bacterial membrane.^[29,30] Upon incubation with the PDI/PFP, redox peaks of PDI/PFP and *M. thermoacetica* appeared simultaneously in the PDI/PFP/*M. thermoacetica* biohybrid system, suggesting the good combination between conjugated

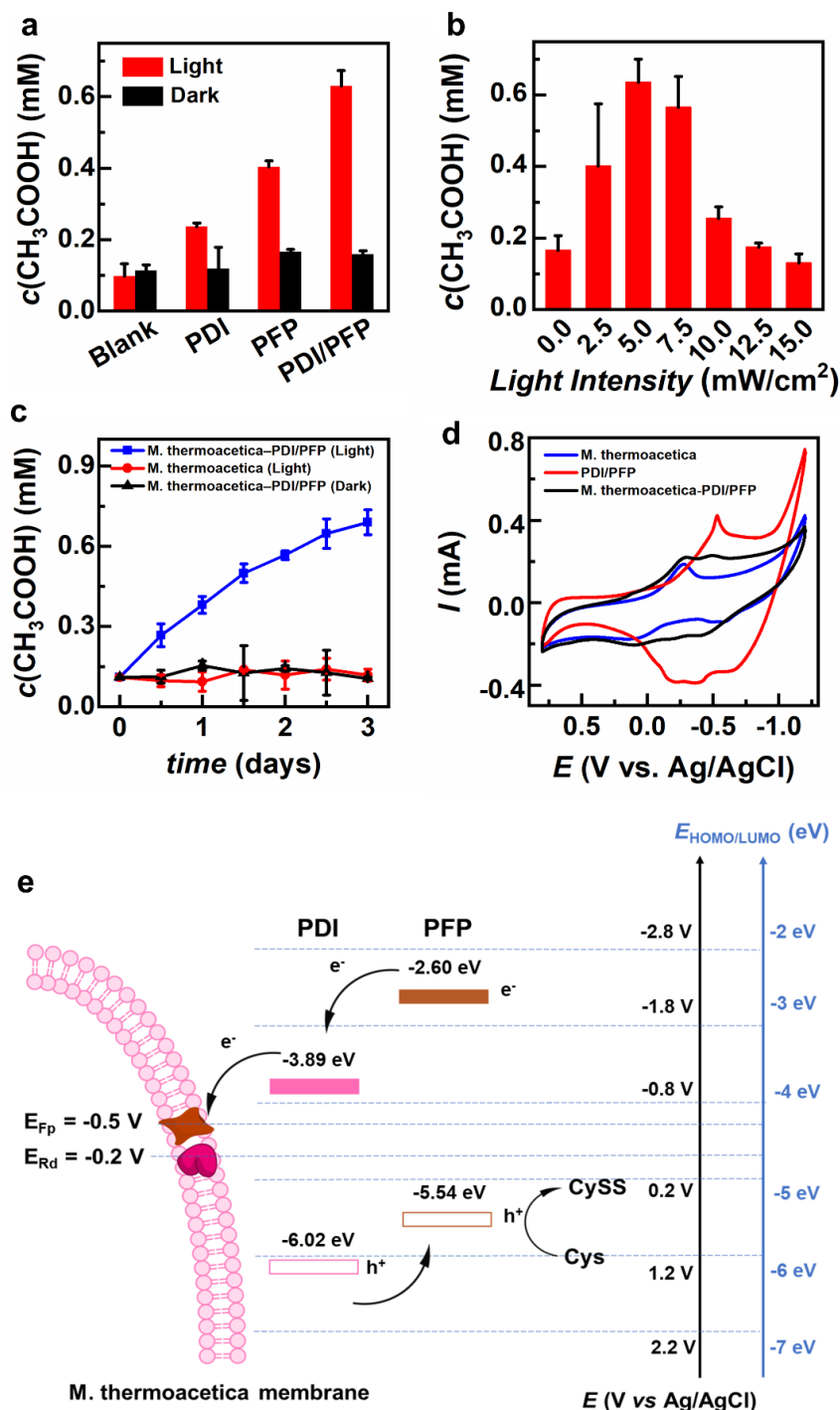


Figure 4. (a) Photosynthetic production of acetic acid by conjugated molecules/*M. thermoacetica* under light and delational controls. (b) The optimal experiment of the light intensity when *M. thermoacetica* incubated with 10 μ M PDI/PFP. (c) The produced acetic acid amount of PDI/PFP/*M. thermoacetica* in an alternating light-dark cycle of 12 hours each. (d) CVs of the *M. thermoacetica*, PDI/PFP, and PDI/PFP/*M. thermoacetica* in 10 mM phosphate buffered saline (PBS) solution (pH=7.4). (e) Energy level diagram of PDI/PFP and the representation of electron transfer mechanism to bacterial membrane.

molecules and bacteria. Furthermore, the reduction potentials of the PDI/PFP were higher than that of the redox mediators Rd and Fp (Figure 4e), ensuring the efficient direct photoexcited-electron transfer from the PDI/PFP heterojunction to membrane proteins.

In summary, we have pioneered π -conjugated organic semiconductor as the photosensitizer to develop a non-photosynthetic bacteria-based photosynthetic biohybrid system for CO₂ reduction. The *p-n* heterojunction (PFP/PDI) exhibited efficient hole/electron separation efficiency and strong light-harvesting ability, as well as good biocompatibility and bioaffinity

with the bacteria. Interestingly, it was found that the positively charged side chains of organic semiconductor PFP could intercalate into bacteria membrane, which is beneficial to the direct transfer of photoexcited electron from PDI/PFP to *M. thermoacetica*. As a result, the electron passed on the Wood-Ljungdahl pathway to synthesize the acetic acid from CO₂. This work is paving a way to explore bioenergy application of organic semiconductors, and also provides a convenient biomanufacturing approach to design organic semiconductor–bacteria biohybrids for efficient solar-to-chemical conversion.

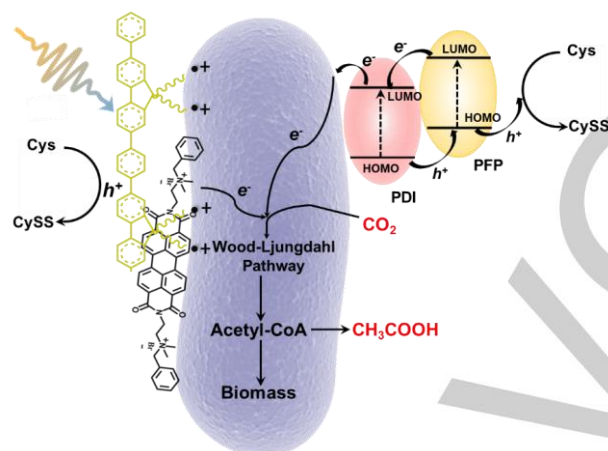
Acknowledgements

The authors are grateful to the financial support from the National Natural Science Foundation of China (Nos. 21533012, 21661132006, and 21605092), and the Special Foundation for Distinguished Taishan Scholar of Shandong Province (ts201511052).

Keywords: organic semiconductors • bacteria • photosynthesis • solar-to-chemical conversion • CO₂ reduction

- [1] K. K. Sakimoto, N. Kornienko, S. Cestellos-Blanco, J. Lim, C. Liu, P. Yang, *J. Am. Chem. Soc.* **2018**, *140*, 1978-1985.
- [2] K. K. Sakimoto, N. Kornienko, P. Yang, *Acc. Chem. Res.* **2017**, *50*, 476-481.
- [3] J. Guo, M. Suástegui, K. K. Sakimoto, V. M. Moody, G. Xiao, D. G. Nocera, N. S. Joshi, *Science* **2018**, *362*, 813-816.
- [4] J. Liu, J. Huang, H. Zhou, M. Antonietti, *ACS Appl. Mater. Interfaces* **2014**, *6*, 8434-8440.
- [5] D. Yang, Y. Zhang, S. Zhang, Y. Cheng, Y. Wu, Z. Cai, X. Wang, J. Shi, Z. Jiang, *ACS Catal.* **2019**, *9*, 11492-11501.
- [6] C. Liu, B. C. Colón, M. Ziesack, P. A. Silver, D. G. Nocera, *Science* **2016**, *352*, 1210-1213.
- [7] K. K. Sakimoto, A. B. Wong, P. Yang, *Science* **2016**, *351*, 74-76.
- [8] H. Zhang, H. Liu, Z. Tian, D. Lu, Y. Yu, S. Cestellos-Blanco, K. K. Sakimoto, P. Yang, *Nat. Nanotechnol.* **2018**, *13*, 900-905.
- [9] M. Miller, W. E. Robinson, A. R. Oliveira, N. Heidary, N. Kornienko, J. Warnan, I. A. C. Pereira, E. Reisner, *Angew. Chem. Int. Ed.* **2019**, *58*, 4601-4605; *Angew. Chem.* **2019**, *131*, 4649-4653
- [10] K. A. Brown, M. B. Wilker, M. Boehm, G. Dukovic, P. W. King, *J. Am. Chem. Soc.* **2012**, *134*, 5627-5636.
- [11] S. F. Rowe, G. Le Gall, E. V. Ainsworth, J. A. Davies, C. W. J. Lockwood, L. Shi, A. Elliston, I. N. Roberts, K. W. Waldron, D. J. Richardson, T. A. Clarke, L. J. C. Jeuken, E. Reisner, J. N. Butt, *ACS Catal.* **2017**, *7*, 7558-7566.
- [12] K. A. Brown, D. F. Harris, M. B. Wilker, A. Rasmussen, N. Khadka, H. Hamby, S. Keable, G. Dukovic, J. W. Peters, L. C. Seefeldt, P. W. King, *Science* **2016**, *352*, 448-450.
- [13] B. Wang, B. N. Queenan, S. Wang, K. P. R. Nilsson, G. C. Bazan, *Adv. Mater.* **2019**, *31*, 1806701.
- [14] C. Zhu, L. Liu, Q. Yang, F. Lv, S. Wang, *Chem. Rev.* **2012**, *112*, 4687-4735.
- [15] Y. X. Wang, L. H. Feng, S. Wang, *Adv. Funct. Mater.* **2019**, *29*, 1806818.
- [16] S. Inal, J. Rivnay, A.-O. Suiiu, G. G. Malliaras, I. McCulloch, *Acc. Chem. Res.* **2018**, *51*, 1368-1376.
- [17] X. Feng, L. Liu, S. Wang, D. Zhu, *Chem. Soc. Rev.* **2010**, *39*, 2411-2419.
- [18] Y. Lyu, J. Tian, J. Li, P. Chen, K. Pu, *Angew. Chem. Int. Ed.* **2018**, *57*, 13484-13488; *Angew. Chem.* **2018**, *130*, 13672-13676
- [19] D. Ghezzi, M. R. Antognazza, M. Dal Maschio, E. Lanzarini, F. Benfenati, G. Lanzani, *Nat. Commun.* **2011**, *2*, 166.
- [20] X. Zhou, L. Zhou, P. Zhang, F. Lv, L. Liu, R. Qi, Y. Wang, M.-Y. Shen, H.-H. Yu, G. Bazan, S. Wang, *Adv. Electron. Mater.* **2019**, *5*, 1800789.
- [21] Y. Wang, S. Li, L. Liu, F. Lv, S. Wang, *Angew. Chem. Int. Ed.* **2017**, *56*, 5308-5311; *Angew. Chem.* **2017**, *129*, 5392-5395.
- [22] P. Zhang, X. Zhou, R. Qi, P. Gai, L. Liu, F. Lv, S. Wang, *Adv. Electron. Mater.* **2019**, *5*, 1900320.
- [23] M. C. Scharber, D. Mühlbacher, M. Koppe, P. Denk, C. Waldauf, A. J. Heeger, C. J. Brabec, *Adv. Mater.* **2006**, *18*, 789-794.
- [24] W. F. Matthew, A. L. Edwin, *Methods Cell Biol.* **2008**, *84*, 79-113.
- [25] K. D. Tarun, C. F. Brewer, *Chem. Rev.* **2002**, *102*, 387-429.
- [26] C. Zhu, Q. Yang, L. Liu, F. Lv, S. Li, G. Yang, S. Wang, *Adv. Mater.* **2011**, *23*, 4805-4810.
- [27] H. Yuan, Z. Liu, L. Liu, F. Lv, Y. Wang, S. Wang, *Adv. Mater.* **2014**, *26*, 4333-4338.
- [28] A. W. D. Larkum, *Curr. Opin. Biotechnol.* **2010**, *21*, 271-276.
- [29] F. Kracke, I. Vassilev, J. O. Krömer, *Front. Microbiol.* **2015**, *6*, 575.
- [30] N. Kornienko, K. K. Sakimoto, D. M. Herlihy, S. C. Nguyen, A. P. Alivisatos, C. B. Harris, A. Schwartzberg, P. Yang, *Proc. Natl. Acad. Sci.* **2016**, *113*, 11750-11755.

In this work, we developed an organic semiconductor-bacteria biohybrid photosynthetic system, which could efficiently realize CO_2 reduction to produce acetic acid through non-photosynthetic bacteria *Moorella thermoacetica*. This work opens a new avenue to explore bioenergy application of organic semiconductors, and also provides a convenient biomanufacturing approach to design organic semiconductor-bacteria biohybrids for efficient solar-to-chemical conversion.



Panpan Gai, Wen Yu, Hao Zhao, Ruilian Qi, Feng Li, Libing Liu, Fengting Lv, and Shu Wang

Page No. – Page No.

Solar-Powered Organic Semiconductor-Bacteria Biohybrids for CO_2 Reduction into Acetic Acid

Accepted Manuscript